NWC-TP-6560

12

Effects of Surface Interactions and Mechanical Properties of PBXs on Explosive Sensitivity

by
E. C. Martin
and
Rena Y. Yee
Research Department

AUGUST 1984

NAVAL WEAPONS CENTER
CHINA LAKE, CA 93555-6001

Naval Weapons Center
AN ACTIVITY OF THE NAVAL MATERIAL COMMAND

FOREWORD

There is a need to reduce the explosive sensitivity of explosives and propellants without sacrificing their energy. We found that the impact sensitivities of some explosives can be changed by surface modification. Propellant studies have also shown that microstructural damage and dewetting have a significant effect on the mechanical properties of the propellant. This study is to investigate the correlation between explosive sensitivity and surface interaction between binder and explosive, and between chemical and mechanical properties of binder and explosive formulation.

This work is funded as a joint effort between the Office of Naval Research (ONR) (Code 432) and Naval Sea Systems Command (NAVSEA) (62R32). The ONR effort is under Task Numbers RR01411 and RR02402 with R. S. Miller as the technical monitor. The NAVSEA effort is under Task Number SR02403 with G. Edwards and H. Adolph as the project managers.

This work was reviewed for technical accuracy by H. P. Richter.

Approved by
E. B. ROYCE, *Head*
Research Department
15 July 1984

Under authority of
K. A. DICKERSON
Capt., U.S. Navy
Commander

Released for publication by
B. W. HAYS
Technical Director

NWC Technical Publication 6560

Published by . . . . . Technical Information Department
Collation . . . . . Cover, 14 leaves
First printing . . . . . 195 copies

UNCLASSIFIED

SECURITY CLASSIFICATION OF THIS PAGE *(When Data Entered)*

REPORT DOCUMENTATION PAGE	READ INSTRUCTIONS BEFORE COMPLETING FORM
1 REPORT NUMBER: NWC TP 6560 — 2 GOVT ACCESSION NO.: AD-A146 368	3. RECIPIENT'S CATALOG NUMBER
4 TITLE *(and Subtitle)*: EFFECTS OF SURFACE INTERACTIONS AND MECHANICAL PROPERTIES OF PBXs ON EXPLOSIVE SENSITIVITY	5. TYPE OF REPORT & PERIOD COVERED: Annual, 1 Oct 82-30 Sep 83
	6. PERFORMING ORG. REPORT NUMBER
7 AUTHOR(s): E. C. Martin and Rena Y. Yee	8. CONTRACT OR GRANT NUMBER(s)
9 PERFORMING ORGANIZATION NAME AND ADDRESS: Naval Weapons Center, China Lake, CA 93555-6001	10 PROGRAM ELEMENT, PROJECT, TASK AREA & WORK UNIT NUMBERS: PE-61153N, Project-RR024-020, RR014-1100, Work Request-N000148 ,WR24159
11 CONTROLLING OFFICE NAME AND ADDRESS: Naval Weapons Center, China Lake, CA 93555-6001	12. REPORT DATE: August 1984
	13 NUMBER OF PAGES: 26
14 MONITORING AGENCY NAME & ADDRESS*(if different from Controlling Office)*	15. SECURITY CLASS. *(of this report)*: UNCLASSIFIED
	15a DECLASSIFICATION/DOWNGRADING SCHEDULE

16 DISTRIBUTION STATEMENT *(of this Report)*

Approved for public release; distribution is unlimited.

17 DISTRIBUTION STATEMENT *(of the abstract entered in Block 20, if different from Report)*

18 SUPPLEMENTARY NOTES

19 KEY WORDS *(Continue on reverse side if necessary and identify by block number)*

Dilatation	Explosives	Polymer Crystallinity
Energetic Polymers	Ignition Characteristics	Explosive Sensitivity
Explosive Sensitivity	Mechanical Properties	Surface Interactions

20. ABSTRACT *(Continue on reverse side if necessary and identify by block number)*

See back of form.

DD FORM 1 JAN 73 1473 EDITION OF 1 NOV 65 IS OBSOLETE

S/N 0102-LF-014-6601

UNCLASSIFIED

SECURITY CLASSIFICATION OF THIS PAGE *(When Data Entered)*

(U) *Effects of Surface Interactions and Mechanical Properties of PBXs on Explosive Sensitivity* by E. C. Martin and Rena Y. Yee. China Lake, Calif., Naval Weapons Center, August 1984. 26 pp. (NWC TP 6560, publication UNCLASSIFIED.)

(U) Much of the first year's effort was spent on materials acquisition, preparation, and characterization. For this study, four binders were selected as the baseline materials. The surface properties of these binders were determined and the results were used to predict the bonding behavior between each binder and RDX. A fracture free energy model was used to predict the bond stability of each RDX-binder system.

(U) Model formulations are being made using the baseline binders. Experimental samples from one mix were sent to evaluators at NWC. The samples were used to determine ignition characteristics, mechanical properties, thermal properties and sensitivity characteristics.

(U) Small preliminary mixes were prepared to determine the concentration of each component in the formulation. Each binder formulation was adjusted to contain similar solid-binder volume ratios. One large energetic formulation was prepared containing RDX and a urethane binder. Experimental samples were prepared from this formulation and shipped to the various investigators. Work performed at NWC included determination of the mechanical and thermal properties, impact sensitivity and various physical properties tests.

(U) A study of the physical properties and crystallinity of BAMO/THF was completed. The surface characteristics of three University of Massachusetts block copolymers are being determined. A multivariate analysis computer program has been obtained for the analysis of the vast array of data being assembled in the program. The utility of this program is being evaluated.

CONTENTS

INTRODUCTION

The objective of this program is to investigate the correlation between explosive sensitivity and the following properties: (1) surface interactions between binder and explosive, and (2) chemical and mechanical properties of binder and explosive formulations.

Plastic bonded explosives (PBX) are mechanical mixtures of explosive crystals with polymeric binders and in some cases plasticizers. Different sensitivity parameters are used to characterize the safety of explosives toward impact, friction, temperature, and electric discharge. There is a need to reduce the explosive sensitivity without sacrificing its energy. A review of the literature suggests that surface properties play a role in desensitization. It has been found in this laboratory that the impact sensitivities of some explosives can be changed by surface modification. Other investigations revealed that the PBX impact sensitivity is related to its viscoelastic dynamic energy loss.* Propellant studies at the Naval Weapons Center (NWC) showed that microstructural damage and dewetting have a significant effect on the mechanical properties of the propellant (Reference 1). Similar effects can be expected to occur in a PBX in that the presence of voids and microcracks due to interfacial debonding, dewetting, and formation of reactive free radicals by molecular bond scission is expected to affect the explosive sensitivity. To determine the influence of the aforementioned factors, the surface properties of the binder and filter should be determined. The surface properties of binders will be determined in both the uncured and cured states. The surface properties of some explosive crystals have been characterized in an earlier program.

Model explosive formulations will be prepared using selected binders and cyclotrimethylenetrinitramine (RDX) or cyclotetramethylenetetranitramine (HMX) having a modified or unmodified crystal surface. The surface interactions will be determined by microscopic examination, dilatation measurements, and dynamic hysteresis studies. The NWC propellant damage energy concept will be applied to define the damage properties and its relation to sensitivity.

*M. Matuszak, Los Alamos Scientific Laboratory, Los Alamos, New Mexico. Private communication, 1981.

Experimental specimens from the model formulations will be sent to Dr. R. Martinson, Lockheed, Palo Alto Laboratory, Palo Alto, Calif., who will carry out small angle X-ray studies, to Prof. J. T. Dickinson, Washington State University, Pullman, Wash., who will conduct fracto emission studies and Prof. K. Kuo, Pennsylvania State University, University Park, Penn., who will investigate the ignition properties. The results obtained by these investigators will be included in the correlation studies.

DISCUSSION

BINDERS

To initiate the program, several binders were selected that are representative of those currently being used in the propellant and explosive areas. Binders that are being qualified were also included. Later, the binders will include the thermoplastic elastomers and other energetic prepolymers as they are developed in the Office of Naval Research (ONR) energy program. The binders being used to establish a data base include hydroxy terminated polybutadiene/isopherone diisocyanate (R45M/IPDI); acrylic polymer; poly(glycidyl azide) (GAP); and bisazidomethyl oxetane/tetrahydrofuran (BAMO/THF).

ENERGETIC FILLERS

The energetic fillers are HMX or RDX. It is known that the various classes of HMX and RDX contain a broad size distribution (Reference 2). It was also shown that filler size and distribution can have large effects on the transient combustion behavior which is believed to play an important role in the deflagration to detonation process (Reference 3).

Production grade RDX and HMX usually contain each other as an impurity. It was decided that several mixes be prepared using pure RDX or HMX to avoid complications. Five pounds of pure RDX and HMX have been received from Los Alamos National Laboratory (LANL), Los Alamos, N. Mex. Since the purification process is time consuming and expensive, no pure explosives will be used after the exhaustion of the pure materials on hand.

RDX RECRYSTALLIZATION

In order to simplify the data interpretation, it was decided to use high energy materials of well defined size distribution. The pure RDX as received had to be recrystallized to obtain suitable particle

sizes. Small quantities of RDX have been successfully recrystallized into 1, 10-20 and 50-100 micron sizes. The 1 micrometer size range was obtained by pouring a 1% acetone solution of RDX into a stirred large volume of water. The 10 to 20 micron size range was produced when a 5% acetone solution of RDX was poured into an equal volume of water. This was the most difficult procedure to reproduce. The solution temperature at time of mixing affects the size and perfections of the crystals. The 50 to 100 micron size was obtained by cooling a saturated solution of RDX in acetone. Time controlled the crystal size. Scale-up of the procedures are in progress.

SCREENING OF PRODUCTION GRADE RDX

A formulation containing a mixture of Class C and Class E RDX showed that the large particles (> 200 microns) had a significant influence on the mechanical properties. In view of this, it was decided to remove the large particles. A batch of Class A RDX was sieved through a number 100 Tyler screen (149 microns).

It is very important to have a thorough knowledge of the particle size distribution for interpretation of the mechanical properties data. A portion of the screened RDX was further screened into five fractions. The original screened RDX and the five fractions were then analyzed. The mean diameter and weight percent of the five fractions are shown in Table 1.

TABLE 1. Particle Size Analysis of Screened RDX.

Screen opening (microns)	Weight percent	Mean diameter (microns)
125-149	21.0	123
105-125	22.6	102
74-105	25.3	78
43-74	18.6	57
43 and under	12.4	...

SURFACE STUDIES

To describe the interactions between the binder and the high energy solids, one must determine the surface properties of the binder and filler in the cured and uncured states. The surface properties of RDX and HMX have been characterized in an earlier program (Reference 4).

In order to measure the direct force of interaction between two neighboring phases, the Wilhelmy plate technique was modified and used for this project (Reference 5). In place of the platinum plate sensor, thin microscope cover glasses coated with the binder of interest are used. The interaction between the binder and the reference liquid is measured by the force required to pull the sensor plate from the pool of the reference liquid. This measurement coupled with independent measurements of the liquid surface tension and density is used to calculate the contact angle of the liquid on the binder. The results agree quite well with those measured by the Sessile drop method (Reference 6).

SURFACE CHARACTERISTICS OF BINDER CURED UNDER DIFFERENT ATMOSPHERES

The binders used in surface characterization are in the form of films. The surface area per volume of binder is large when compared to that in the composite used in other tests. To study this effect, the polyurethane binder samples have been cured under vacuum, nitrogen, and air. No difference was observed in their reflective infrared spectra although their surface characteristics are quite different as shown in Figure 1. This suggests that the surface layers investigated in the surface study are very thin compared with the usual thickness of about 1 micron detected by the infrared. The atmospheric effect should be considered in the preparation of samples for evaluation.

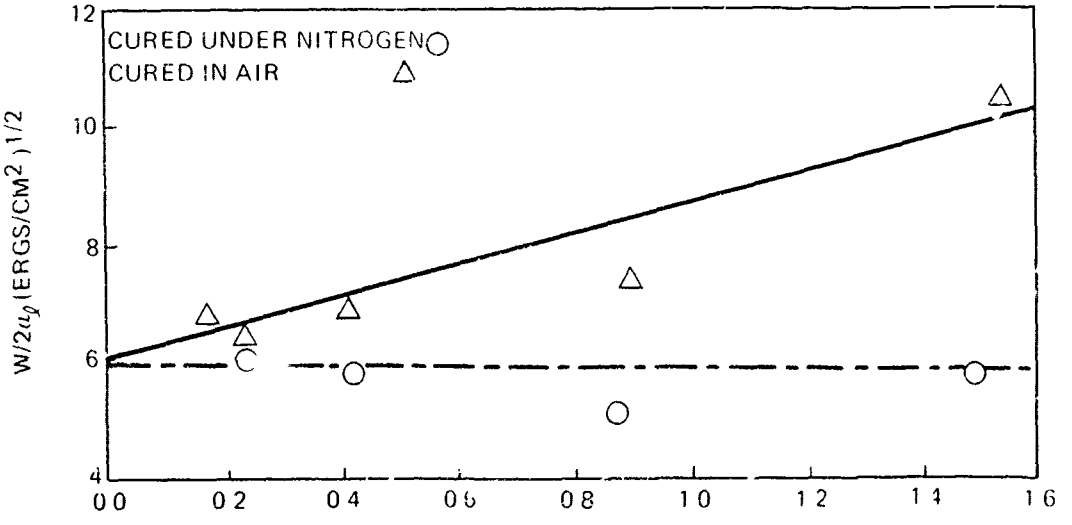

FIGURE 1. Environmental Effect on Surface Free Energies of R45M/IPDI.

SURFACE CHARACTERISTICS DURING DIFFERENT STAGES OF BINDER CURE

The surface properties of the cured binder are usually considered in the study of adhesion. However, it is the consensus that one considers the initial wetting of the ingredients and the adhesion in the cured stage. The complicating factor is that the ingredients change from liquids to solid during the curing process. It is necessary to change the surface characterization methods for the liquids and the solids. The very viscous liquids prevent the utilization of some measuring techniques. The method that has been selected is the Sessile Drop Method. The usual series of reference liquids are used on the cured binders for their surface characterization. The reference materials for the liquids are polyethylene and polymethyl methacrylate. The polyethylene represents a nonpolar surface and the polymethyl methacrylate represents a polar surface. The measured contact angles are listed in Table 2.

TABLE 2. Contact Angles of Liquid Polymers on Reference Solids.

Liquid	Contact angle, degrees	
	Polyethylene	Polymethyl methacrylate
R45M	32.7	25.2
R45M/IPDI (1/2 to 1 hour ambient)	32.2	21.2
R45M/IPDI (2 to 2-1/2 hours, ambient)	32.1	23.8

Since R45M is the major ingredient (more than 92%), it is included. The contact angles of the uncured polymer on polyethylene is very similar to that of R45M. This indicates that the London dispersive force of interaction is similar in the uncured polymer to that of R45M. The addition of IPDI decreases the contact angle on the polymethyl methacrylate. They increase with the curing time. This trend is parallel to the amount of the polar IPDI in the sample.

WETTABILITY OF SELECTED BINDERS

The four binders selected for the baseline study are an acrylic binder containing vinyl pyrrolidone, R45M/IPDI, GAP, and BAMO/THF. The contact angles of several reference liquids on the aforementioned cured binders and others that are included in the program are listed in Table 3.

TABLE 3. Contact Angles of Various Binders.

Liquid binder	Water	Formamide	Methylene iodide	Tetrabromo ethylene	Aroclor 1242
	γ_ℓ[a] = 72.8	γ_ℓ = 58.3	γ_ℓ = 50.8	γ_ℓ = 49.7	γ_ℓ = 45.3
BAMO/THF	61.4	64.2	23.1	26.2	24.2
Acrylic polymer	63.2	51.4	41.9	42.3	20.5
EVA[b]	69.4	63.8	...	37.5	19.7
R45M/IPDI	109.0	94.0	52.0	...	46.0
GAP	90.3	70.7	63.5	38.8	35.9
PEPU[c]	102.8	80.8	46.2	45.6	37.2
PEPI-1210[d]	94.0	68.2	33.2	29.8	46.5
PEPI-1210H	94.0	78.7	39.3	35.5	43.0

[a] γ_ℓ = surface tension in dynes/cm.

[b] Ethylene-vinyl acetate copolymers.

[c] Polyether-polyurethane.

[d] Polyether-polyimide.

Three thermoplastic elastomers sent to us from the University of Massachusetts, Amherst, Mass., are a polyether-polyurethane block polymer (PEPU), a polyether-polyimide block polymer (PEPI-1210), and a polyether-polyimide block polymer with 5% di-hydroxyethyl hydantoin. The bonding agent has been incorporated into the backbone of PEPI-1210H to enhance wetting. Since the contact angles seemed to be the same as those of PEPI-1210, the hydantoin has not changed the wetting behavior. One possible explanation is that the hydantoin structure is not at the surface and thus not effective. If such is the case, locating the hydantoin in the side chain instead of the backbone may make some difference.

The method of Kaeble (Reference 7) is used for the surface free energy analysis. In this method, the results from all reference liquids are averaged to obtain one set of free energy values for each binder. The main equations of this analysis are:

$$\gamma_{\ell v} = \gamma^D_{\ell v} + \gamma^P_{\ell v} = \alpha_1^2 + \beta_1^2 \qquad (1)$$

$$\gamma_{sv} = \gamma_{sv}^{D} + \gamma_{sv}^{P} = \alpha_s^2 + \beta_s^2 \tag{2}$$

$$\gamma_{sv} = \gamma_s - \tau_e \tag{3}$$

$$W_a = \gamma_{\ell v}(1 + \cos\theta) \leq 2\gamma_{\ell v} \tag{4}$$

$$W_a = 2(\alpha_\ell \alpha_s + \beta_\ell \beta_s) \tag{5}$$

$$\frac{W_a}{2\alpha_\ell} = \alpha_s + \beta_s(\beta_\ell/\alpha_\ell) \tag{6}$$

where

v, ℓ, s = vapor, liquid, and solid

$\gamma_{\ell v}$ = surface free energy of liquid-vapor interface

γ_{sv} = surface free energy of solid-vapor interface

γ^D = dispersive force component of surface free energy

γ^P = polar force component of surface free energy

$\alpha = (\gamma^D)^{1/2}$

$\beta = (\gamma^P)^{1/2}$

τ = equilibrium spreading pressure

W_a = work of adhesion

θ = contact angle

According to Equation 6, when $W_a/2\alpha_\ell$ is plotted against β_ℓ/α_ℓ, the intercept should be α_s and the slope, β_s. The results are shown in Figure 2. The urethane binder is the least polar system. The data for the BAMO/THF and the acrylic binders are very close. They are also

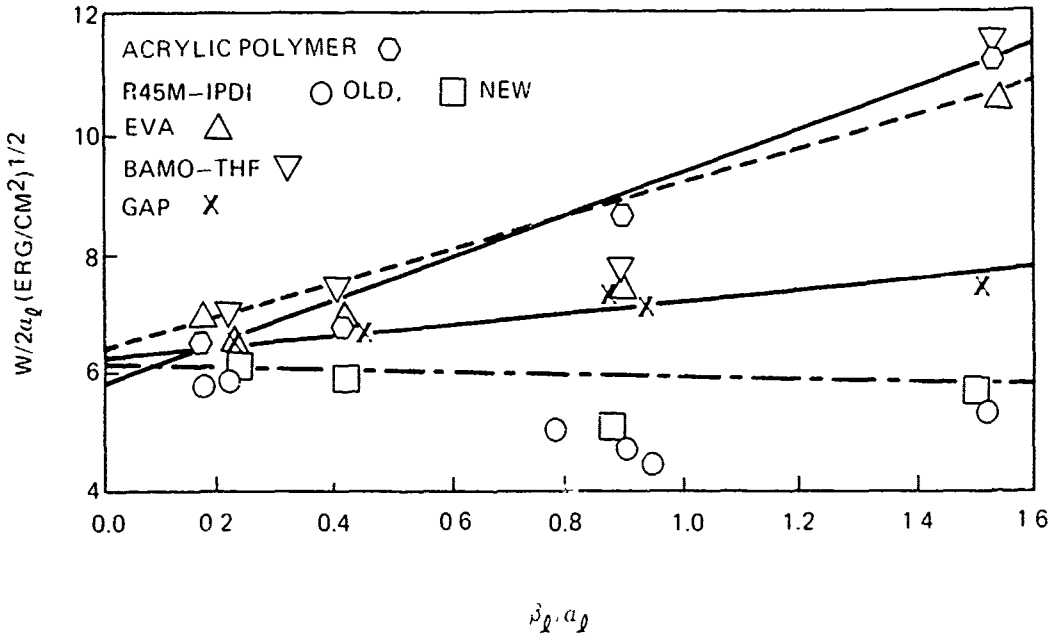

FIGURE 2. Surface Analysis of Binders.

very close to those of RDX. The results obtained for the University of Massachusetts thermoplastic elastomers are shown in Figure 3. The α_s and β_s values are read from Figures 2 and 3 and the values of γ_s^D and γ_s^P are the squares of α_s and β_s, respectively. These values are listed in Table 4. γ_s is the total surface free energy (sum of γ_s^D and γ_s^P). The last column of Table 4 is a term called "polarity" of the system. It shows the percentage of contribution of the polar free energy to the total surface free energy of the binder.

It was surprising to find that the PEPU and PEPI samples show such low polarity. Both the R45M/IPDI and PEPU systems are polyurethanes and one might expect to see some similarities. The PEPI, however, is expected to be more polar. It is speculated that the procedure of test sample preparation may affect the morphology of the surface. After a long discussion with the researchers of the University of Massachusetts, it was decided that test samples prepared next to a more polar medium than air will be studied.

The γ_s^D values for most of the systems are very close except for the paraffin and KEL-F. This reflects the similar London dispersive

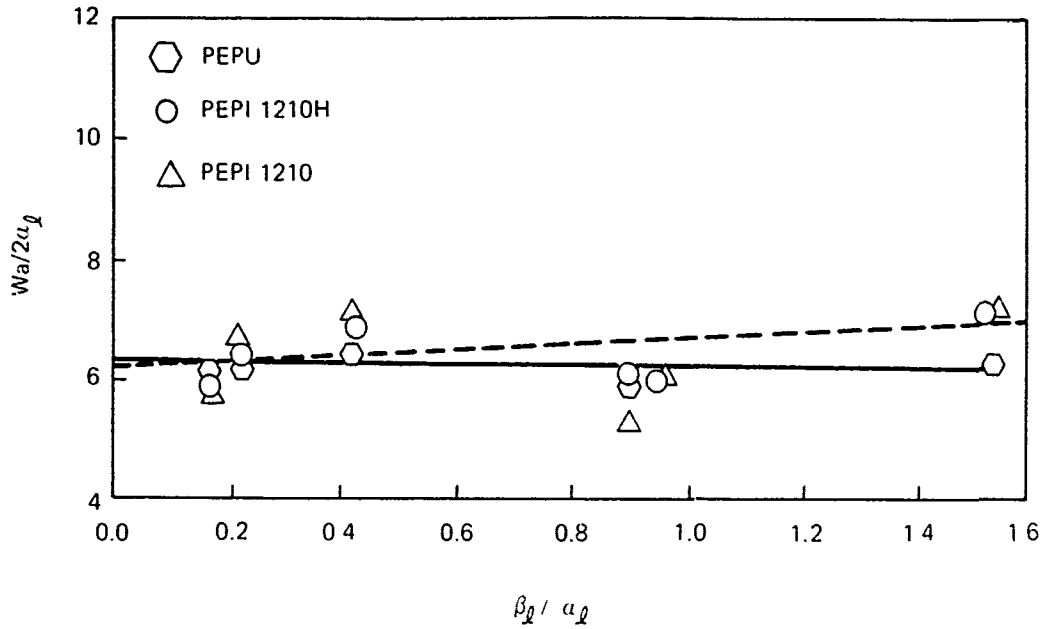

FIGURE 3. Surface Analysis of New Block Copolymers.

forces of the backbones of the polymers. The variations are observed in the γ_s^P terms which show the different polar nature of the polymers. The same trend is shown in the polarity values. The values of the BAMO/THF and acrylic binders are very close to those of RDX and therefore they are probably better binders for RDX in terms of surface properties. The idea is better demonstrated in the interfacial tension and work of adhesion values between the binder and RDX as listed in Table 5.

The work of adhesion is calculated from Equation 6. The geometrical mean method is used to calculate the interfacial tension. When two materials are joined by an interface, the more similar the two materials are, the lower the interfacial tension will be and the better the adhesion will be between them. Therefore, it is desirable to have a low interfacial tension between the solid and the binder. The BAMO/THF and acrylic binder appear promising in this respect. The work required to separate the interface is called the work of adhesion; the more work required to separate the two phases, the better adhesion. The same two binders also appear promising in this case.

TABLE 4. Free Energy Analysis of Polymers and RDX.

Material	γ_s^D	γ_s^P	γ_s	γ^P/γ_s
RDX	36.0	12.2	48.2	0.254
BAMO/THF (5-1)	38.4	12.4	50.8	0.224
Acrylic polymer	33.6	12.2	47.8	0.266
EVA	39.6	6.9	46.5	0.148
Polyethlyene terephalate	37.8	3.5	41.3	0.085
Polystyrene	40.0	0.6	41.0	0.015
PEPU	41.0	0.05	41.0	0.001
GAP-N100	39.8	0.8	40.6	0.020
R45M/IPDI	38.4	0.8	39.2	0.020
PEPI(1210)	38.4	0.8	39.2	0.020
PEPI(1210H)	38.4	0.8	39.2	0.020
Paraffin	25.4	0.0	25.4	0.000
KEL-F	21.9	2.9	24.8	0.117

TABLE 5. Interfacial Tension and Work of Adhesion Between RDX and Polymers.

Polymers	Interfacial tension dynes/cm	Work of adhesion ergs/cm^2
BAMO/THF	0.04	99.0
Acrylic polymer	0.04	94.0
EVA	0.82	93.8
PET	2.63	86.2
Polystyrene	7.56	82.2
GAP	6.95	82.2
R45M/IPDI	6.66	80.8
PEPI	9.06	80.5
PEPU	10.83	78.3
KEL-F	4.94	66.0
Paraffin	13.00	60.0

FRACTURE FREE ENERGY AND SURFACE FREE ENERGY

It is believed that the mechanical properties of a filled system are influenced by the binder-filler interface. The Griffith's fracture free energy can be related to surface free energies (References 7 and 8). The relationships are shown below:

$$\sigma_G = (2E/\pi C)^{1/2}(R^2 - R_o^2)^{1/2} \tag{7}$$

$$R_o^2 = 0.25(\alpha_1 - \alpha_3)^2 + (\beta_1 - \beta_3)^2 \tag{8}$$

$$R^2 = (\alpha_2 - H)^2 + (\beta_2 - K)^2 \tag{9}$$

$$H = 0.5(\alpha_1 + \alpha_3) \tag{10}$$

$$K = 0.5(\beta_1 + \beta_3) \tag{11}$$

where

σ_G = critical crack tip propagation stress

E = Young's modulus

C = crack length

α_1, β_1 = surface properties of one component of the interface

α_3, β_3 = surface properties of the second component of the interface

α_2, β_2 = surface properties of the material acting as debonding agent

π = surface energy reduction due to immersion in ambient vapor phase

Kaeble's surface energy diagram can be used to graphically predict the adhesion between two phases (Reference 9). In this method, the square root of the dispersive and polar surface free energies (α and β, respectively) are plotted. The α and β values of the baseline binders and some other materials are listed in Table 6.

TABLE 6. Surface Free Energies.

Material	α	β	Material	α	β
RDX	6.0	3.5	Ethylene glycol	5.59	4.36
Water	4.67	7.14	Formamide	5.68	5.09
Hexane	4.30	0.0	Aroclor 1242	6.63	1.14
Ethanol	4.12	2.32	Methylene iodide	6.96	1.82
Acrylic polymer	5.8	3.5	Polymethyl methacrylate	6.0	2.07
R45M/IPDI	6.2	0.9	PS[a]	6.4	0.77
EVA	6.3	2.62	Teflon	3.5	1.22
Paraffin	5.04	0.0	PET[b]	6.1	1.87
GAP	6.3	0.9	BAMO/THF	6.20	3.52

[a]Polystyrene.

[b]Poly(ethylene terephthalate).

The values listed in Table 6 are plotted in Figure 4. In order to predict the adhesion between RDX and any one of the materials, e.g., polystyrene, draw a circle through the two points. The distance between the center of the circle and the origin of the coordinates should be equal to the R term in Equation 9. The diameter of the circle should be equal to the term R_o in Equation 8. If a third material is inside of the circle, it would debond the interface. According to the points in Figure 4; the aroclor 1242 point inside the RDX-polystyrene circle would debond the interface. Since the ethanol point is outside of the circle, it would not debond the interface. Therefore, the smaller the circle, the less chance of having a third phase within the circle. It would be less likely debonded. According to this model, the BAMO/THF and the vinyl acrylic binders are the most suitable in terms of their surface free energies.

CHARACTERIZATION OF BAMO/THF

A new lot of BAMO/THF (lot 5-L) was received from M. Frankel at the Rocketdyne Division, Rockwell International, Canoga Park, Calif. This material had a lower viscosity than the previously received lot 5-2. To determine the causes of this variation and to characterize the materials on hand, the properties of two lots of BAMO/THF copolymers, poly-bis(azidomethyl)oxetane (poly-BAMO) and polytetrahydrofuran) (poly-THF) were studied. The techniques used to accomplish this include optical and polarizing microscopy, ^{13}C nuclear magnetic resonance (NMR) X-ray diffraction, and differential scanning calorimetry (DSC). The results are summarized in Table 7.

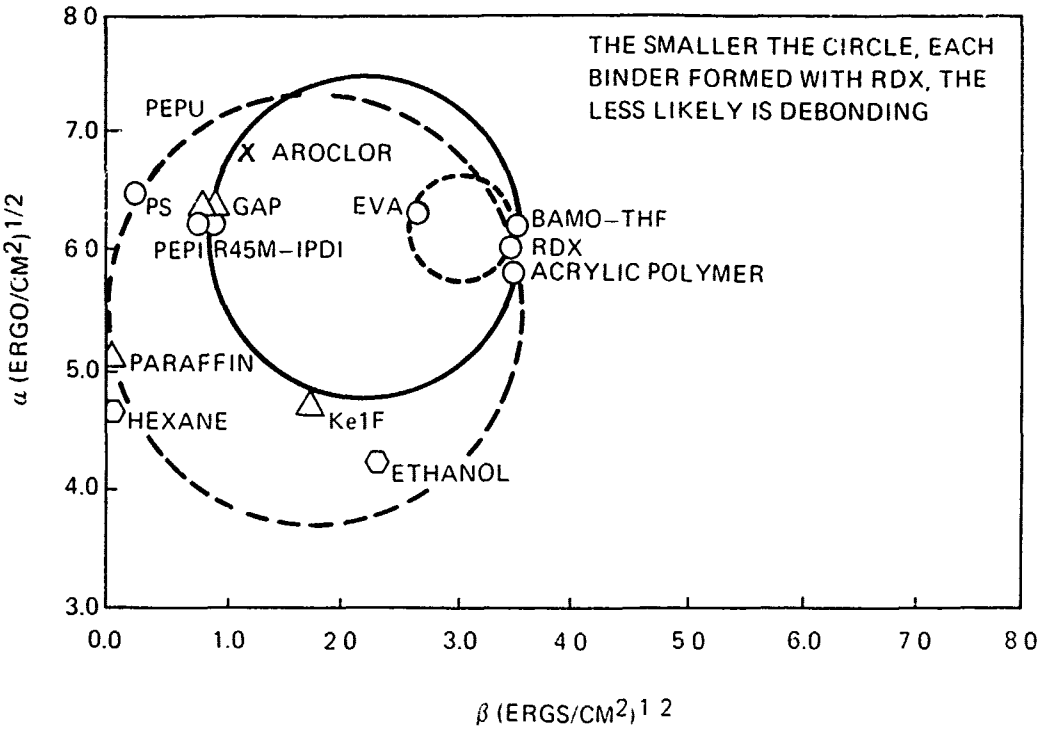

FIGURE 4. Surface Energy Diagram.

CRYSTALLINITY IN BAMO/THF

The BAMO/THF lot 5-2 has a higher viscosity than lot 5-L. This has been explained as the result of crystallinity. Our X-ray diffraction results confirm this point and provide further information on the nature of the crystallinity. The radial scans of poly-BAMO, BAMO/THF lots 5-2 and 5-L are shown in Figure 5. According to their X-ray patterns, poly-BAMO is a crystalline material as shown by the intensities of the peaks and their sharpness. The BAMO/THF lot 5-L shows only one very broad amorphous peak. Therefore, it is not crystalline or the degree of crystallinity is too low to be detected by X-ray. The X-ray scan of BAMO/THF lot 5-2 shows some small peaks on top of the broad amorphous peak. The three peaks in BAMO/THF lot 5-2 (2θ = 16.3, 19.5, and 23.6 degrees) corresponds to the three stronger peaks in poly-BAMO (2θ = 16.6, 19.4, and 23.9 degrees). It is difficult to draw specific conclusions from only three peaks, especially when the structures of

TABLE 7. Properties of Two Lots of BAMO/THF.

Properties	BAMO/THF 5-2	BAMO/THF 5-L
M_W	4022	5156
M_N	2578	3662
Eq wt	1210	1864
Appearance	Thick gel	Gel
Flow tendency	Flows at 40°C	Flows at 40°C
NMR	More homo sequence	Less homo sequence
Microscopic observations	Volume filled with small spherulites (melting point 40°C)	A few larger spherulites (melting point 40°C)
X-ray	Slightly crystalline	No crystallinity

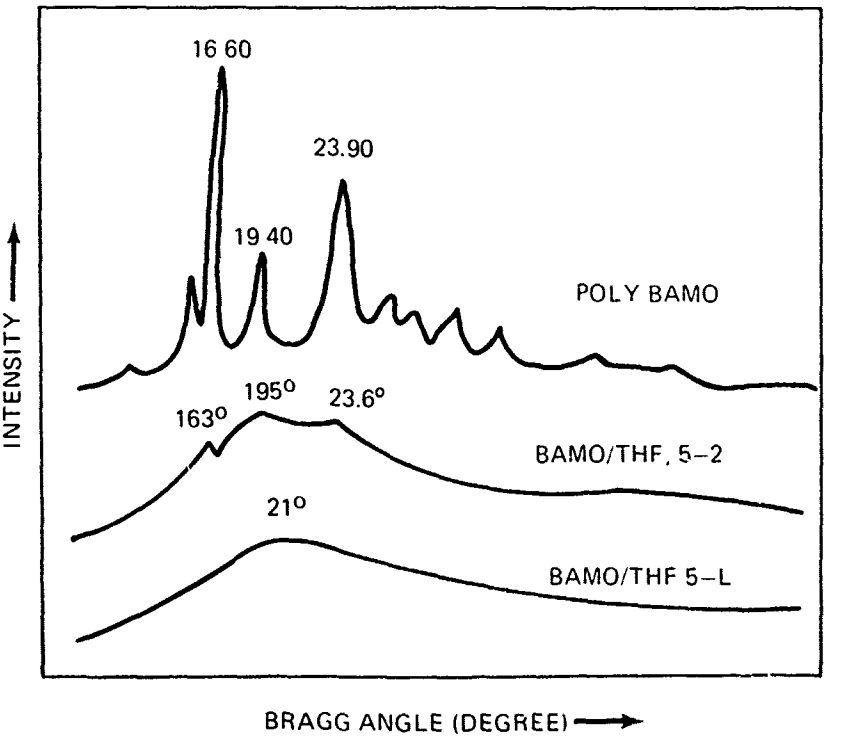

FIGURE 5. X-Ray Radial Scan of BAMO Polymers.

the corresponding unit cell have not been determined. It suggests that the crystallinity in the BAMO/THF lot 5-2 is due to the BAMO homo sequence because the three peaks correspond to those obtained for the homopolymer. The ^{13}C NMR data also supports this idea. The NMR spectra show that lot 5-2 contains more THF-THF sequences than lot 5-L. Since the two lots contain about the same molar ratio of BAMO, it implies that lot 5-2 also contains more BAMO-BAMO sequences and thus it is easier to form the crystalline segments.

The presence of crystalline material is further substantiated by the crystalline spherulitic structure observed under the crossed polaroids of a microscope. Lot 5-L contains 10 to 20 volume percent of 25-micron diameter spherulites. Lot 5-2 contains a large volume percent of small spherulites (~10 to 15 microns in diameter). In copolymers, the percent of crystallinity can be very low. These results show that even though no crystallinity was observed in the X-ray of the lot 5-L material, a very small amount is present. When the two lots of BAMO/THF were heated on a hot stage under the microscope, the spherulites were seen melting at 40 to 44°C. This temperature corresponds to the melting peak observed in the DSC which will be discussed later. The viscosities of these materials decrease above their melting points as indicated by the fact that they flowed above the melting temperature. It is believed that the viscosity of BAMO/THF copolymers is associated with the crystallinity which in turn originated from the presence of homo BAMO sequence in the crystalline phase.

THERMAL PROPERTIES OF BAMO/THF

The thermal properties of BAMO/THF copolymers were determined by DSC using a DuPont 1090 instrument. These include the glass transition temperature (T_g) and melting temperature (T_m) which were obtained in the same run in an open aluminum pan under nitrogen atmosphere and at 5°C/minute heating rate. The exothermic peaks were determined in closed aluminum pans under air atmosphere and at 10°C/minute heating rate. The results are collected in Table 8. The poly-THF and poly-BAMO are also included for comparison.

Both lots of BAMO/THF thermally decompose around 257°C. This is very close to the decomposition of poly-BAMO. This indicates that the azido group breaks down before the THF group. The heat of fusion of the two lots of BAMO/THF are very low. This indicates that the molar ratio of BAMO in these two lots are similar since most of the initial heat of fusion is from the BAMO group. The fast decomposition of the azido containing material is demonstrated by the inverted exothermic peak in a DSC run at 20°C/minute heating rate (Figure 6). The heat generated in the thermal decomposition was so fast, it raised the temperature of the cell above its programmed heating rate. After the decomposition, the heat flow stopped and the cell dropped back to a

TABLE 8. Thermal Properties of BAMO/THF and Their Homopolymer.

	THF	BAMO/THF (lot 5-2)	BAMO/THF (lot 5-L)	BAMO
Exothermic peak (°C)	410	257	257	261
Heat of decomposition (Joule/gram)	Small and gradual	1827	1874	2486
T_m (°C)	11 and 17	36-42	35-41	84
Heat of fusion (Joule/gram)	69.2	1.3	0.6	45.4
T_g (°C)	(-85 and -45)	-55	-58	...

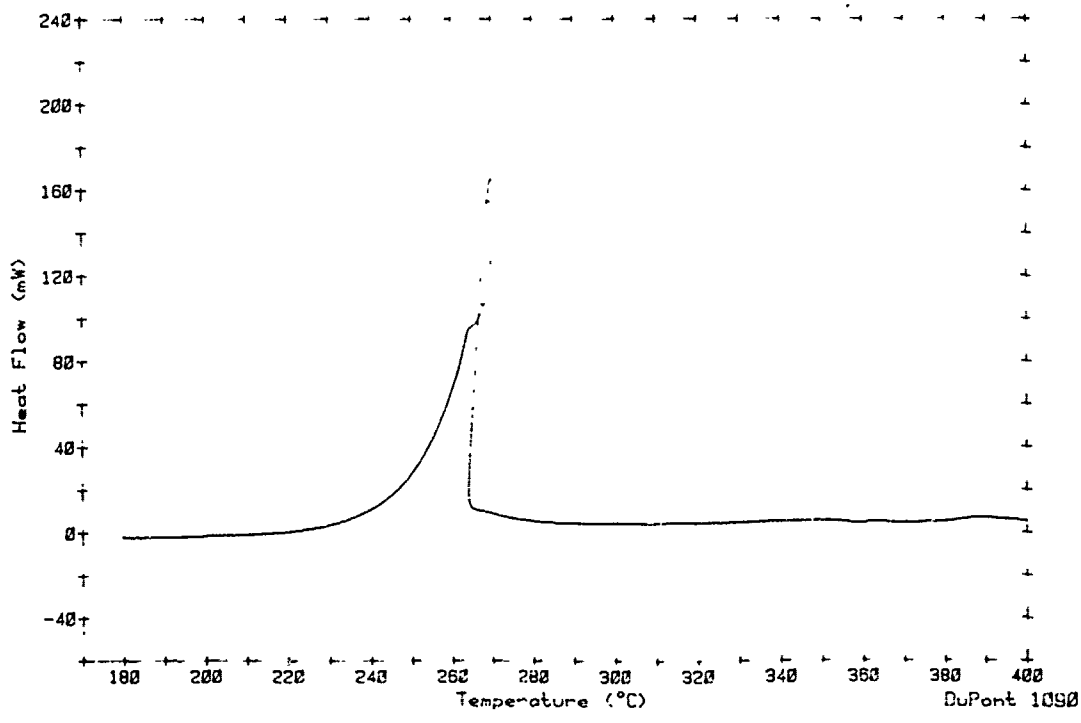

FIGURE 6. Differential Scanning Calorimetry of Poly-BAMO.

lower temperature as shown by the temperature going in the reverse direction. It is interesting to note that HMX also shows this phenomenon when tested under the same conditions.

The poly-BAMO has a melting point (T_m) of 84°C and the poly-THF has double peaks at 11 and 17°C. The melting point of the two lots of BAMO/THF are in between which is to be expected. The fact that the heat change in the DSC curve indicating the melting of BAMO/THF is so small in comparison with that of the homopolymers (1:45) suggests that the degree of crystallinity is very low in the copolymer. This also agrees with the ease of melting and low degree of crystallinity observed. The melting temperature is essentially the same as the melting temperature of spherulites observed under the microscope on the hot stage. The glass transition temperature (T_g) of BAMO/THF lot 5-2 and 5-L are -55 and -58°C, respectively. The difference is real because the T_g curves have been duplicated in repeated runs. The lot 5-2 being more viscous and more crystalline, should also show higher T_g. The T_g of a gumstock from lot 5-L cured with N-100 is -48°C. This also follows the same reasoning that the mobility of the polymer chains is more restricted in the gumstock than in the 5-L prepolymer and thus higher T_g. Two transition temperatures were observed in the DSC curve of poly-THF. The nature of this double peak has not been explored.

INERT FORMULATIONS

Several inert formulations were prepared for preliminary testing. In these formulations the binder was R45M/IPDI and the filler was sodium chloride or glass beads. The surface of the glass beads was either cleaned by annealing or silanized using γ-aminopropyltriethoxysilane. Because the formulations contained 80% solids which resulted in a high mix viscosity, the early formulations contained an unacceptable amount of voids. The problem was solved by shaking the mixture under vacuum to remove the bubbles before heat curing the mixture. A good sample tested by the hydrolytic bulk compression method contained only 0.3% voids. Test specimens of these materials were sent to Washington State University and Lockheed for evaluation.

ENERGETIC FORMULATIONS

One energetic formulation was prepared for evaluation. The binder, R45M cured with IPDI, contained 75% RDX. The RDX mixture consisted of 22.5% Class C and 52.5% Class E. Microscopic examination revealed that the Class C contained a significant amount of particles in the 200- to 800-micron size range. The cured formulation was cut

into test specimens and distributed to the evaluators at NWC. Test specimens were not sent to Washington State University, Pennsylvania State University, or Lockheed because the explosive shipping exemption had not been received from the Department of Transportation (DOT). An interim exemption was later received from Naval Sea Systems Command and will be used until the exemption is received from DOT.

Table 9 lists the mechanical properties tests that will be conducted on each formulation. Figure 7 shows the typical mechanical properties data that are obtained when evaluating a propellant under shear deformation. Figure 8 shows the torsional shear results obtained with the R45M/IPDI formulation (BLX-1). The low maximum stress and onset of dewetting is caused by the presence of large (200 to 800 microns) RDX particles in the formulation.

TABLE 9. Scheduled Mechanical Tests.

Uniaxial tension - Young's modulus, loss tangent tensile dilatation
Dynamic hysteresis - E', E'', tan ϕ, viscoelastic energy loss dissipates into heat
Fracture toughness - resistance to crack propagation
Dynamic mechanical analysis - T_g, low temperature properties
Torsional shear - shear dilatation, onset of dewetting, failure stress and strain
Hydrostatic compression - void content and bulk modulus

The hydrostatic compression properties for one specimen of BLX-1 are shown in Figure 9. The results show that the initial void content of the formulation was 2.7% and the bulk modulus was 6.3×10^5 psi.

A comparison of the tensile and shear deformation of BLX-1 is shown in Table 10. The initial moduli obtained in both tests are quite close based on theory. Likewise, the stress at the onset of dewetting and maximum stress are comparable. The data shows that the strain at failure and the stress at failure are no longer comparable for the two tests. However, this is to be expected because the samples in shear or tension dewet at different rates beyond the onset of dewetting.

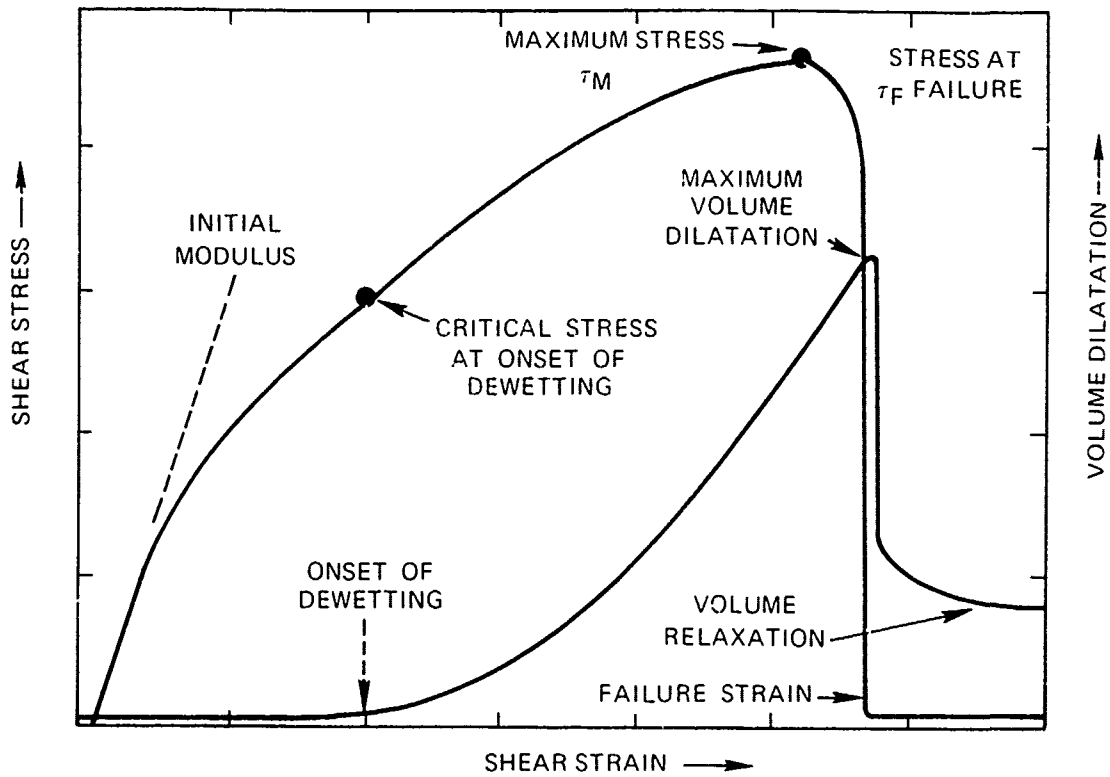

FIGURE 7. Mechanical Properties of a Solid Propellant Under Shear Deformation.

The ignitability characteristics of BLX-1 are listed in Table 11. At the listed energy input levels, the times to detect first light and the times required to completely consume the specimens suggests that the formulation has suitable ignition characteristics.

The burn rate data for BLX-1 are listed in Table 12. It is realized that the low values are due to an insufficient amount of oxidizer in the formulation. However, the data will be incorporated in the data matrix for comparison with other data base systems.

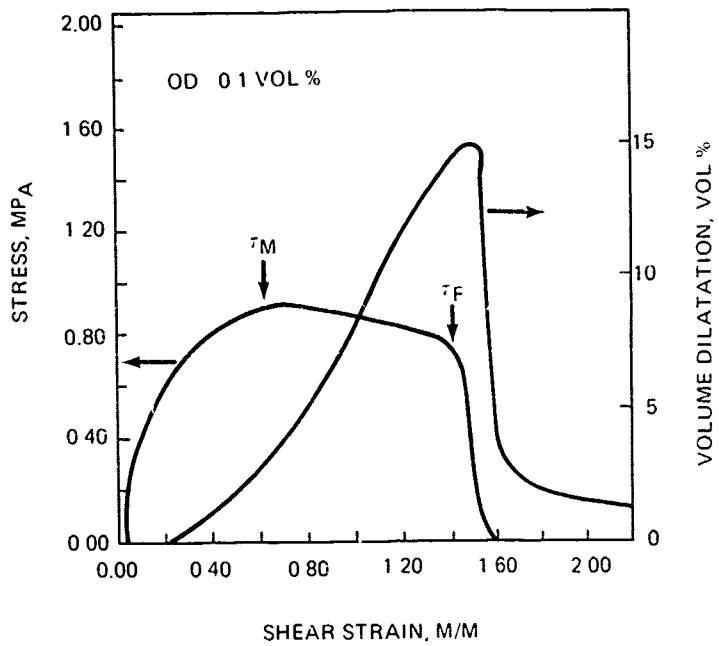

FIGURE 8. Torsional Shear Study of R45M/IPDI RDX Formulation (BLX-1).

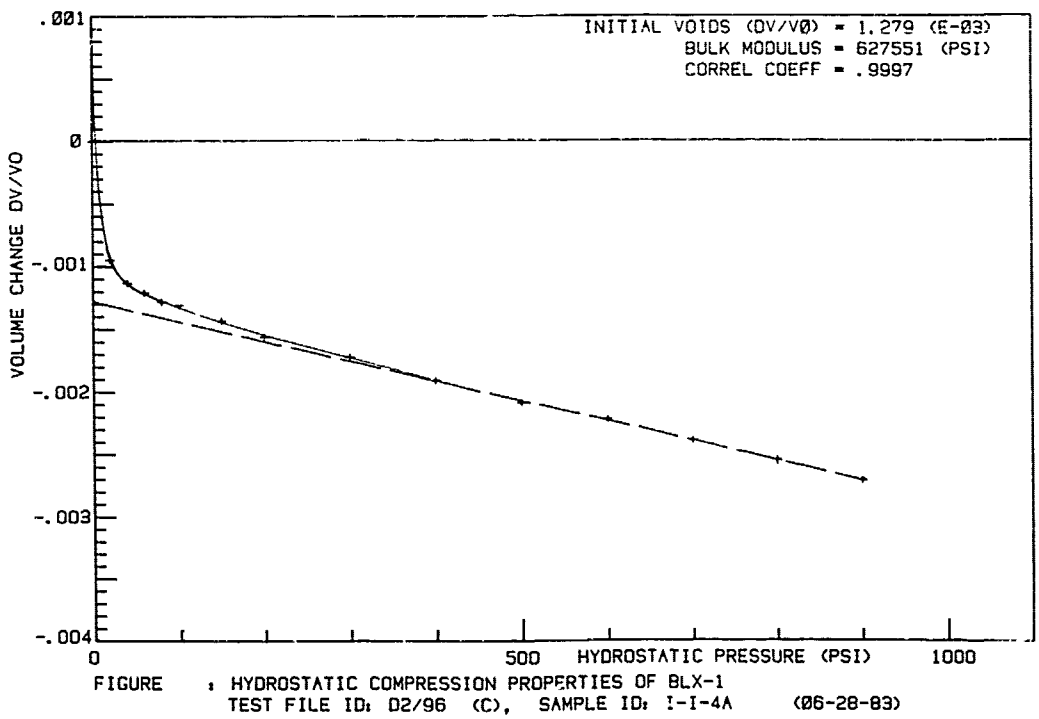

FIGURE 9. Hydrostatic Compression Properties of BLX-1.

TABLE 10. Comparison of Tensile and Shear Deformation of R45M/IPDI RDX Formulation (BLX-1).

	Tensile	Shear
Initial modulus (MPa)	15.2	5.0
Stress at onset of dewetting (MPa)	0.699	0.674
Maximum stress (MPa)	0.860	0.928
Strain at failure (m/m)	0.132	0.149
Stress at failure (MPa)	0.860	0.731
Maximum volume change (%)	3.5	15.0

TABLE 11. Ignitability of R-45M/IPDI RDX Formulation at 250 psia (BLX-1).

Cal/cm^2s	First light (ms)	Go/no-go (ms)
60	15.9 ±0.89	18.2 ±0.6
100	6.1 ±0.51	10.3 ±0.9
150	2.4 ±0.24	5.4 ±0.7
200	1.1 ±0.13	4.5 ±0.9

TABLE 12. Burn Rate Study of R-45M/IPDI RDX Formulation (BLX-1).

Psia (N_2)	Burn rate (in/sec)
100	0.042
400	0.096
600	0.114
800	0.132
1000	0.165
1300	0.187

CONCLUSIONS

Several inert formulations were prepared and forwarded to Prof. J. T. Dickinson (WSU) and Dr. R. Martinson (Lockheed, Palo Alto Laboratory) for evaluation. Prior to preparing a large model formulation, small hand mixes were made to establish the composition of the formulations. Experience has shown that caution must be used when using this technique.

The surface characteristics of the baseline binders indicated that the acrylic polymer and the BAMO/THF binder would bond better to RDX than would GAP or the R45M/IPDI binder. The microfracture free energy model also predicts that the acrylic polymer and the BAMO/THF copolymer form a strong bond with RDX.

In order to compare the four baseline binders, their model formulations should have a minimum of variables. Therefore, the formulations were designed to have similar solid-binder volume ratios. Even though the binders used in the baseline study have been evaluated in a number of established formulations, these formulations cannot be used in this study because they contain ingredients that will alter the surface chemistry when compared to the surface chemistry data obtained for the binder. Model mixes have shown that omitting one ingredient from the formulation can drastically affect the mechanical properties. This suggests that the surface chemistry of the system plays an important role during processing.

The surface analysis studies of three new thermoplastic elastomers from the University of Massachusetts have been initiated. Preliminary results show that the work of adhesion is similar to that obtained with the R45M/IPDI binder. The effect of sample preparation on surface morphologies is being investigated to determine how this affects the work of adhesion.

The physical properties of two lots of BAMO/THF have been characterized. The differences in viscosity from batch to batch has been shown to be associated with the amount of homo block and its degree of crystallinity.

REFERENCES

1. A. H. Lepie and A. Adicoff. "Dynamic Mechanical Behavior of Highly Filled Polymers. Energy Balance and Damage." J. Appl. Polym. Sci., Vol. 18 (1974). pp. 2165-2176.

2. C. F. Price and T. L. Boggs. "The Effects of Sample Particle Size and Distribution on Transient Combustion," Propulsion Systems Hazards Meeting, April 1982, Naval Weapons Center, China Lake, Calif.

3. T. L. Boggs and others. "Role of Gas Phase Reactions in Deflagration-to-Detonation Transition," The Seventh Symposium (International) on Detonation, Preprint Vol. I, June 1981, pp 85-93.

4. R. Y. Yee, A. Adicoff and E. J. Dibble. "Surface Properties of HMX Crystal," presented at 17th JANNAF Combustion Meeting, Hampton, Virginia, 22-26 September 1980. 17th JANNAF Combustion Meeting, Vol. 2, pp 461-468, 22-26 September 1980, CPIA Publication 329, November 1980.

5. A. E. Alexander in "Physical Methods of Orgonic Chemistry," A. Weissberger, Ed., 3rd ed., p. 732, Interscience, New York, 1959.

6. W. D. Hawkins. "The Physical Chemistry of Surface Film." Reinhold, New York, 1952.

7. D. H. Kaeble, P. J. Dynes and E. H. Cirlin. "Interfacial Bonding and Enviromental Stability of Polymer Matrix Composites." J. Adhesion, 6 (1974), p. 23.

8. D. H. Kaeble and P. J. Dynes, "Surface Energy Analysis of Treated Graphite Fibers." J. Adhesion, 6 (1974), p. 239.

9. T. Smith. "Surface Energy and Adhesion." J. Adhesion, 11 (1980), p. 243.

INITIAL DISTRIBUTION

5 Naval Air Systems Command
- AIR-03P25, B Sobers (1)
- AIR-310C, H Rosenwasser (1)
- AIR-330, R Brown (1)
- AIR-7226 (2)

12 Chief of Naval Research, Arlington
- ONR-260, D. Siegel (1)
- ONR-413, R. S Miller (10)
- ONR-432, N. L Basdekas (1)

5 Naval Sea Systems Command
- SEA-09B312 (2)
- SEA-62R2 (1)
- SEA-62R32 (1)
- SEA-64E, R Beauregard (1)

1 Assistant Secretary of the Navy (Research, Engineering and Systems, L. V Schmidt, Rm 5E 731)
1 Commander in Chief, U.S. Pacific Fleet (Code 325)
1 Headquarters, U.S. Marine Corps (Code RD-1, A L Slafkosky, Scientific Advisor)
1 Commander, Third Fleet, Pearl Harbor
1 Commander, Seventh Fleet, San Francisco
1 David W Taylor Naval Ship Research & Development Center Detachment, Annapolis (G. Bosmajian, Applied Chemistry Division)
2 Naval Academy, Annapolis (Director of Research)
1 Naval Explosive Ordnance Disposal Technology Center, Indian Head (Code D, L. Dickinson)
1 Naval Ocean Systems Center, San Diego (J McCartney)
1 Naval Ocean Systems Center, Marine Sciences Division, San Diego CA (S Yamamoto)
2 Naval Ordnance Station, Indian Head
- Code 5253, S. Mitchell (1)
- Code PM4, C L Adams (1)

2 Naval Postgraduate School, Monterey
- R. A. Reinhardt, Physics & Chemistry Department (1)
- W Tolles, Dean of Research (1)

3 Naval Research Laboratory
- Code 6030, J Karle (1)
- Code 6100 (1)
- Code 6510, J. Schnur (1)

1 Naval Ship Systems Engineering Center, Philadelphia (J. Boyle, Materials Branch)
3 Naval Ship Weapon Systems Engineering Station, Port Hueneme
- Code 5711, Repository (2)
- Code 5712 (1)

3 Naval Surface Weapons Center, Indian Head Detachment, Indian Head
- Code R101, G. L. Mackenzie (1)
- Code R16, T. D. Austin (1)
- R. Gill, Bldg 600 (1)

10 Naval Surface Weapons Center, White Oak Laboratory, Silver Spring
- Code R04, D. J. Pastine (1)
- Code R10D, H G. Adolph (1)
- Code R11
  - C. Gotzmer (1)
  - T. Hall (1)
  - M. J. Kamlet (1)
  - K. F. Mueller (1)
- Code R121, M. Stosz (1)
- Code R122, L. Roslund (1)
- Code R13
  - R Bernecker (1)
  - E. Zimmet (1)

1 Naval War College, Newport
1 Naval Weapons Station, Yorktown (L. R. Rothstein, Assistant Director, Naval Explosives Development Engineering Department)
1 Naval Weapons Support Center, Crane (Code 50C, B. Douda)
1 Office of Naval Research, Boston Branch Office (L. Peebles)
1 Office of Naval Research, Pasadena Branch Office (R. J Marcus)
1 Office of Naval Research, San Francisco Branch Office (P. A. Miller)
2 Office of Naval Technology, Arlington
    MAT-0712, LCDR J. Walker (1)
    MAT-0716, A. Faulstich (1)
4 Strategic Systems Project Office
    Code SP2731, Propulsion Unit (1)
    Code SP27314, M. Baron (1)
    J. F. Kincaid, Rm. 901 (1)
    E. L. Throckmorton, Rm. 1048 (1)
1 Army Armament Research and Development Command, Dover (DRDAR-LCE, R. F. Walker)
2 Army Missile Command, Redstone Arsenal
    DRSMI-R, R. G. Rhoades (1)
    DRSMI-RK, W. Wharton (1)
4 Army Ballistic Research Laboratory, Aberdeen Proving Ground
    DRDAR-BLI
        I. W. May (1)
        L. A. Watermeier (1)
    DRDAR-BLP, A. W. Barrows (1)
    DRDAR-BLT, P. Howe (1)
1 Army Research Office, Research Triangle Park (Chemical & Biological Sciences Division)
1 Ballistic Missile Defense Advanced Technology Center, Huntsville (D. C. Sayles)
1 Air Force Adademy, Colorado Springs (FJSRL/NC, J. S. Wilkes, Jr.)
1 Air Force Armament Division, Eglin Air Force Base (AFATL/DLDL, O. K. Heiney)
1 Air Force Intelligence Service, Bolling Air Force Base (AFIS/INTAW, Maj. R. Lecklider)
2 Air Force Office of Scientific Research, Bolling Air Force Base
    Directorate of Aerospace Sciences, L. H. Caveny (1)
    Directorate of Chemical Sciences, D. L. Ball (1)
1 Air Force Rocket Propulsion Laboratory, Edwards Air Force Base (AFRPL/LKLR, S. Shackelford)
1 Air Force Rocket Propulsion Laboratory, Edwards Air Force Base (AFRPL/MKP, R. Geisler MS 24)
1 Air Force Rocket Propulsion Laboratory, Edwards Air Force Base (AFRPL/MKPA, F. Roberto)
12 Defense Technical Information Center
1 Aerojet Strategic Propulsion Company, Sacramento, CA (R. L. Lou), Via AFPRO
1 Anal-Syn Laboratory, Inc., Paoli, PA (V. J. Keenan)
1 Atlantic Research Corporation, Gainesville, VA (W. D. Stephens)
1 Atlantic Research Corporation, Alexandria, VA (M. K. King)
1 British Embassy, Defence Equipment Staff (A. S. Sinden, Munitions Directorate, Propellants and Explosives)
2 California Institute of Technology, Pasadena, CA
    W. G. Knauss, Graduate Aeronautical Laboratory (1)
    N. W. Tschoegl, Department of Chemical Engineering (1)
1 Catholic University of America (T. Litovitz, Physics Department)
1 Cornell University, School of Chemical Engineering, Ithaca, NY (F. Rodriguez)
1 Fluorochem, Inc., Azusa, CA (K. Baum)
1 Georgia Institute of Technology, Atlanta, GA (E. Price, School of Aerospace Engineering)
2 Hercules Incorporated, Allegany Ballistics Laboratory, Cumberland, MD
    Aerospace Division
        J. O. Hartman (1)
        R. C. Musso (1)
1 Hercules Incorporated, Eglin Air Foce Base (AFATL/DLDL, R. L. Simmons), Via AFPRO
2 Hercules Incorporated, Magna, UT
    E. H. Debutts (1)
    J. H. Thacher (1)